

Adaptive changes of extracellular amino acid concentrations in mouse dorsal striatum by 4-AP-induced cortical seizures

Terumi Nagai¹, Norio Takata^{1,2}, Yoshiaki Shinohara¹, and Hajime Hirase^{1,3*}

1.

RIKEN Brain Science Institute
Wako, Saitama, Japan

2.

Current address: Department of Neuropsychiatry, School of Medicine, Keio University, Shinjuku, Tokyo, Japan.

3.

Saitama University Brain Science Institute
Saitama, Saitama, Japan

Published as:

[Nagai T, Takata N, Shinohara Y, Hirase, H. \(2015\) Adaptive changes of extracellular amino acid concentrations in mouse dorsal striatum by 4-AP-induced cortical seizures. *Neuroscience*. \(2015\), 295:229-236.](#)

DOI: [10.1016/j.neuroscience.2015.03.043](#)

* Correspondence should be addressed to Hajime Hirase; email: hirase@brain.riken.jp

Keywords

HPLC, GLT-1, GLAST, basal ganglia, cortical seizures

Abbreviations

4-AP 4-aminopyridine GLAST, glutamate/aspartate transporter; GLT-1, glutamate transporter 1; HPLC, High-performance liquid chromatography; LFP local field potential MSNs medium spiny neurons PVDF polyvinylidene difluoride

Acknowledgements: This work was supported by the RIKEN Brain Science Institute, KAKENHI grants (23115522, 25115726, 26117520, and 26282222) from the Ministry of Education, Culture, Sports, Science, and Technology of Japan, and the Human Frontier Science Program (RGP0036/2014). We thank Prof. Kohichi Tanaka (Tokyo Medical and Dental University) for an advice on immunoblotting and Dr. Akiko Shimamoto (Meharry Medical College) for discussion. We are grateful to Drs. Hiromasa Morishita and Nobuko Mataga, as well as the Support Unit for Bio-Material Analysis, RIKEN BSI Research Resources Center for help with HPLC analysis.

Abstract

The striatum is a major target of cerebral cortical output. The cortico-striatal projection has been well described, however, the neurochemical changes that occur in the striatum after prolonged cortical hyperactivation remain to be investigated. In this study, extracellular levels of glutamate, GABA, and alanine levels were measured in the dorsal striatum using microdialysis in anesthetized mice at resting condition and during 4-aminopyridine (4-AP)-induced cortical seizures. After topical application of 4-AP on the primary motor cortex that induced cortical seizures, the extracellular level of striatal GABA increased by 40% in sixty minutes. By contrast, the extracellular level of striatal glutamate decreased by 20%. Moreover, the surface amounts of striatal glutamate/aspartate transporter (GLAST) and glutamate transporter 1 (GLT-1), the major astrocytic high-affinity glutamate transporters, tended to increase by cortical seizures in 60 min, suggesting a recruitment of the glutamate transporters from internal stores. 4-AP also resulted in a steady increase of alanine levels which are thought to reflect glutamate and pyruvate metabolism in neurons and astrocytes. These observations possibly delineate adaptive changes of striatal metabolism by severe cortical seizures.

Introduction

Cortical seizures cause devastating clinical conditions such as uncontrollable limb movement and loss of consciousness (Banerjee et al., 2009, also Epilepsy Foundation fact sheets, <http://www.epilepsy.com/learn/about-epilepsy-basics>, last reviewed in March 2014). The non-selective voltage-gated potassium channel blocker 4-aminopyridine (4-AP) has been used to induce seizures in the rodent brain for both *in vitro* and *in vivo* studies (for example, Yamaguchi and Rogawski, 1992; Luhmann et al., 2000). While the extracellular levels of neurotransmitters have been investigated at seizure foci using experimental animals (Timmerman and Westerink, 1997), fewer studies examined the efferent areas of a seizure locus.

The striatum is a telencephalic structure involved in the planning and execution of motor movement (Grillner et al., 2005, for review). The major afferents of the striatum are the dopaminergic projection from the pars compacta of the substantia nigra and the glutamatergic projection from the cerebral cortex and thalamus, forming the nigrostriatal, corticostriatal and thalamostriatal pathways, respectively. Many cortical areas including sensory and motor areas project to the striatum (Gerfen, 2004; Wilson, 2004). Layer 5 pyramidal neurons are the principal cortical cells that give rise to afferents to the striatum (Hedreen, 1977; Jones et al., 1977) and form synapses on GABAergic medium spiny neurons (MSNs) (Hersch et al., 1995) which represent more than 90% of striatal neurons. In addition to extra-striatal projection, MSNs have extensive recurrent collaterals that innervate MSNs and interneurons, thus making the circuit largely GABAergic (Gerfen, 2004; Wilson, 2004). There is an ambient level of GABA whose origin is likely to be neurons, as TTX attenuates the tonic GABA current in slices (Ade et al., 2008).

Although the anatomy and physiology of the corticostriatal projection have been investigated for decades, the effect of cortical seizures on the striatum is largely unknown. In the current study, we measured the extracellular levels of glutamate, GABA and alanine in the dorsal striatum after 4-AP-induced cortical seizures in anesthetized mice. We find that the seizure induction in the primary motor cortex leads to a gradual decrease of extracellular glutamate and a concomitant increase of GABA, which could be explained by increases of surface glial glutamate transporters. In addition, we observed a robust accumulation of extracellular alanine, possibly reflecting

pyruvate metabolism.

Material and methods

All experimental protocols were approved by the RIKEN Institutional Animal Care and Use Committee and conform to the National Institutes of Health Guide for the Care and Use of Laboratory Animals (National Research Council).

Local Field potential (LFP) recording and cortical seizure induction

Adult male C57BL/6J mice were anesthetized with urethane (1.6 g/kg) and placed in a stereotaxic apparatus. The scalp was surgically removed and the skull was exposed for craniotomy and durotomy. The body temperature was maintained at 37 °C by a heat pad with feedback temperature control (TR-200, FST, Foster City, CA, USA). LFP recording from the motor cortex was performed using a borosilicate glass pipette (resistance 2~3 MΩ) containing physiological saline inserted approximately 350 μm below the pial surface (AP +1.7 mm, ML -0.5 mm from bregma). LFP was measured by taking a differential signal between the microelectrode and a reference signal at the neck of the animal. The LFP signal was amplified by 1,000 fold and bandpass filtered between 0.1 and 4 kHz (Multiclamp 700B, Molecular Devices, CA, USA), which was digitized at 25 kHz using a commercial data acquisition card (BNC-2110, National Instruments, TX, USA). The data acquisition software was written with LabView (National Instruments, TX, USA). Cortical seizure induction was made by topical application of 50 mM 4-AP (in HEPES ACSF) onto a pial area ranging ML -1.0 to -2.0 mm and AP 0.7 – 2.0 mm. The 4-AP solution was sustained by a piece of Gelfoam.

c-Fos immunohistochemistry

Sixty minutes after topical application of 4-AP, five adult male mouse brains were perfusion-fixed by a fixative (4% paraformaldehyde in 0.1M phosphate buffer, pH 7.4). The brains were post-fixed in the same fixative solution for up to three days. Coronal sections containing the striatum were made using a microslicer (Pro-7 Linear Slicer, Dosaka EM, Kyoto, Japan) in 0.1M phosphate buffer. Slices were immunostained with a c-Fos antibody (Calbiochem P38, 1:3000). Biotinylated secondary antibody was used

and the signal was further amplified by the ABC kit (1:400, PK-6100, Vector Laboratories, CA, USA). Finally, the signal was visualized by a standard nickel-enhanced DAB method. c-Fos positive cells were counted manually using a BX-51 Olympus upright microscope.

In vivo microdialysis

A straight-shaped cellulose dialysis probe (1.0 mm in length, 350 μm outer diameter, 50,000 Da cutoff, A-I-4-01, EICOM Co. Ltd., Kyoto, Japan) was slowly inserted into the striatum (AP +0.3 mm, ML -2.3 mm, DV 3.0 mm from the pia; AP and ML coordinates were adjusted ± 0.1 mm depending on the surface vasculature pattern) of anesthetized mice. The probe was equilibrated for at least 120 min while perfusing with 2 $\mu\text{l}/\text{min}$ HEPES-ACSF. Consecutive dialysate samples were collected in 10-min bins. After probe stabilization, three dialysate samples were collected as control and five dialysate samples were collected after seizure induction. *In vitro* recovery for dialysis probes was determined by placing the probes in HEPES-ACSF that contained known concentrations of GABA and glutamate at a flow rate of 2 $\mu\text{l}/\text{min}$. Consecutive 10-min samples were collected, yielding the recovery rate of 6.3%. After completion of the dialysis experiments, the location of the dialysis probe was verified with Nissl-stained 60 μm -thick serial coronal sections.

High-performance liquid chromatography

A HPLC column switching system with pre-column derivatization was used for GABA, glutamate, and alanine analyses in microdialysate samples according to previous methods (Mataga et al., 1991; Hensch et al., 1998). For derivatization of free amino acids, o-phthalaldehyde OPA solution was prepared immediately before the HPLC analysis as follows: 5mg OPA (27824-61, Nacalai, Japan) was first dissolved in 200 μl methanol and then 5 μl 2-mercaptoethanol (2-ME, 21438-82, Nacalai) and 800 μl of 0.1 M Na_2CO_3 (199-01585, Wako, Japan) were added. The OPA solution was set in the reagent vial position in an autosampler (M-500, EICOM, Japan). The sample was automatically mixed for 2 min with an equal volume of OPA solution, totaling to 30 μL , by the autosampler at room temperature and half of the derivatized sample was injected to the HPLC immediately. Injected samples were then divided into two components

using a 6-way bulb autoinjector (EAS-20s, EICOM), equipped with two pumps for mobile phases A and B (L-2130, HITACHI, Tokyo, Japan), an autosampler, a trap column (COSMOSIL Guard 5C18-MS-II, 4.6 mm ID × 10 mm), and two analysis columns at 36 °C (COSMOSIL 5C18-MS-II, 4.6 mm ID × 150 mm), that are capable of high throughput detection with fluorescent detectors (wavelengths: excitation 340 nm, emission 440 nm) (GL-7453A, GL Science and L-7480, EICOM). Mobile phases are composed of 0.1 M citrate buffer, 0.2 M phosphate buffer, water, and acetonitrile with volume ratios of 169:331:380:120 (pH 6.4) for A and 222:278:250:250 (pH 5.9) for B, respectively. The flow rate was set at 1.1 ml/min. The mobile phase in the trap column was switched from mobile phase A to B after 90 seconds and switched back to A after 12 minutes. Glutamate was eluted in mobile phase A and GABA and alanine were detected in mobile phase B within 15 minutes.

Data were acquired by the Power Chrom system (EPC-500, EICOM). Spectral peak quantification and the following analyses were done using custom Matlab (Mathworks, MA, USA) programs. Probe stabilization was first checked by analyzing the 120 min recovery period. Once the equilibration is confirmed, the following three dialysate samples were collected to determine the basal concentrations of respective compounds. *In vitro* recovery for dialysis probes was determined by placing the probes in HEPES-ACSF that contained known concentrations of glutamate and GABA at a flow rate of 2 µL/min to collect consecutive 10-min samples. The detection limits of GABA, glutamate and alanine were 0.002, 0.002, 0.005 pmol/µL, respectively. Part of data on basal glutamate level was published in a recent paper (Aida et al., 2015)

Glutamate transporters immunoblotting

Sixty minutes after topical application of 4-AP onto a pial area ranging ML -1.0 to -2.5 mm and AP 0.0 to 2.0 mm, the brains of the mice were rapidly removed from the skull and the striatum was immediately dissected and cooled in an plastic tube containing ice-cold HEPES-buffered 0.32 M sucrose with 5mM CaCl₂, 10 mM MgCl₂ with proteinase inhibitor cocktail (cOmplete mini, Roche, Mannheim, Germany). The same part of the brain was removed from non-treated mice (anesthetized for the same amount of time as the 4-AP group) for control. Each sample was homogenized within a few minutes from the extraction of the striatum using a homogenizer (Polymix PX-SR 90D,

Kinematica, Luzern, Switzerland). Nuclear fractions are removed by $800 \times g$ centrifugation (10 min, 4 °C). Subsequently, crude synaptosomal and Golgi fractions were removed by taking the supernatant after $20,000 \times g$ centrifugation (20 min, 4 °C). The membrane fraction was separated by collecting the precipitate after $100,000 \times g$ centrifugation (1 hour, 4 °C) and dissolved in 0.5% SDS HEPES-buffered solution. The protein concentration was measured by the BCA method (Pierce Biotechnology, Rockford, IL, USA). A fixed protein amount of 220 ng per sample was subjected to SDS-PAGE using 5-20% gradient acrylamide gel (e-PAGEL SPG-520L, Atto, Tokyo, Japan) and transferred to polyvinylidene difluoride (PVDF) membrane (Sequi-Blot, BioRad, Hercules, CA, USA; 280 mA, 16 hours). The PVDF membranes were reacted with anti-GLT-1 (rabbit, Af670-1, Frontier Institute, Ishikari, Japan) or anti-GLAST (rabbit, Af660-1, Frontier Institute) antibodies overnight at 4 °C. For enhanced chemiluminescence detection, secondary antibody conjugated with horseradish peroxidase (NA9340, GE Healthcare, Little Chalfont, UK) and Western Lightning Plus ECL (PerkinElmer, Waltham, MA, USA) were used. Images were obtained by LAS-3000 (Fuji Film, Tokyo, Japan), and analyzed by the MultiGauge software.

Statistical Analysis:

All measured values are expressed as mean \pm S.E.M. Statistical tests are computed by Matlab with Statistics Toolbox and described as comparisons are made in the results section.

Results

Basal levels of extracellular amino acids were determined from six consecutively sampled dialysates after at least two hours of settling time from the dorsal striatum (Figure 1A). HPLC readouts of GABA, glutamate, and alanine were stable for the six samples per experiment with coefficients of variation of 0.179 ($n = 12$ animals), 0.0828 ($n = 13$), 0.0718 ($n = 10$), respectively (Figure 1B). The basal levels of these amino acids were calculated by using a recovery rate calibration of 3.01%, 2.41%, and 3.84% for GABA, glutamate, and alanine, respectively. As a result, the basal concentrations were computed as GABA: 247 ± 106 nM; glutamate 1141 ± 223 nM; alanine 4180 ± 1065 nM (Figure 1C).

Next, we induced cortical seizures by topically applying 4-AP (50 mM), a non-selective antagonist of voltage-gated potassium channels, to the craniotomy for the primary motor cortex. Seizures were induced within several minutes after topical application of 4-AP as observed by the LFP recordings from the motor cortex (Figure 2A). Full blown seizure events occurred intermittently in the beginning with an interval of 1-3 min, and later became more frequent or sometimes the seizures occurred continuously. The root square mean (RMS) amplitude of the LFP (bin width = 5 minutes) shows that the seizure reaches to a plateau state after 20 min (Figure 2B, n = 9 animals). To investigate if the cortical seizure induction has resulted in an increased neuronal activity in the striatum, c-Fos expression was examined by immunohistochemistry in a separate group of five mice (Figure 2C). In all examined cases, the seizure induction side had a higher density of c-Fos-positive cells than the contralateral side (269.3 ± 49.1 vs. 89.9 ± 17.2 cells/mm², $p < 0.05$, paired t-test, Figure 2D).

As unilateral application of 4-AP activates the ipsilateral striatum, amino acid concentrations were measured in the ipsilateral striatum during cortical seizures. As shown in Figure 3, there were significant changes of GABA, glutamate and alanine after topical application of 4-AP on the motor cortex. The GABA level started to increase 20 min after 4-AP application and reached to on average 143% of control level for at 50 min (Figure 3A, n = 7 animals). By contrast, the glutamate level was decreased to 79% after 50 min (Figure 3B, n = 8). The extracellular levels of GABA and glutamate were both highly significant ($p < 0.001$; 1-way ANOVA followed by the Tukey-Kramer *post-hoc* tests) for time points after 40 minutes. Notably, the alanine level constantly increased after 20 minutes (Figure 3C, n = 7 animals). The alanine levels were measured to be 147%, 198%, 239%, and 284% at 20, 30, 40, and 50 min, respectively; these values are all statistically significant ($p < 0.001$; 1-way ANOVA followed by the Tukey-Kramer *post-hoc* tests). As the extracellular glutamate level was decreased by 60 min of cortical seizures, we asked whether the surface glutamate transporter expression has altered. Western blotting of two major glial glutamate transporters, GLT-1 (SLC1A2) and GLAST (SLC1A3), on the membrane fraction of post-cortical seizure striatum revealed that both GLT-1 and GLAST tended to have higher surface expression than the control (Figure 4, GLT-1: 13% increase in 4-AP samples, $p = 0.03$, t-test;

GLAST: 12% increase, $p = 0.26$; $n=6$ animals for both 4-AP and control).

Discussion

Our measurements of mouse striatal glutamate and GABA levels were comparable to previously published values by Lada et al. (1998) or Kennedy et al. (2002), despite the species and anesthetic differences (glutamate: 1141 vs. 920 or 1760 nM; GABA 247 vs. 270 nM). Previous striatal microdialysis studies have focused on amino acid concentration changes after neuronal excitation by local infusion of neurostimulants (Morales-Villagrán and Tapia, 1996; Segovia et al., 1997; Kennedy et al., 2002) or after generalized seizure induction by systemic administration of 4-AP (Kovács et al., 2003). Our approach is distinguished from these previous studies as we investigate the effect of cortical seizures on the striatum. Our approach is also different from a previous study that used fast microdialysis (5 s interval) that detected an immediate increase of the striatal glutamate level after a brief stimulation of the prefrontal cortex in that our measurements represent steady-state amino acid levels with longer sampling time. The difference of neuronal activity between the cortical seizures and generalized seizures is manifested by the c-Fos expression pattern. First, in our study, the striatal c-Fos expression was highly biased to the ipsilateral side (Fig. 2). Next, the c-Fos expression in the ipsilateral hippocampus was modest (Fig. 5). Hence, the c-Fos expression induced by topical 4-AP application on the motor cortex is contrasted with that of generalized seizures in which prominent and widespread c-Fos expression is reported including the striatum and hippocampus of both hemispheres (Barone et al., 1993; Willoughby et al., 1995).

We demonstrate that the GABA levels increased whereas the glutamate level decreased after the seizure induction in the motor cortex. As striatum has extensive functional GABAergic local collaterals from MSNs (Chuhma et al., 2011), it is conceivable that the GABA level increases with the cortical glutamatergic drive. Previous studies with local neurostimulant infusion or generalized seizures reported increases of striatal glutamate (Rowley et al., 1995; Morales-Villagrán and Tapia, 1996; Segovia et al., 1997; Peña and Tapia, 2000; Kovács et al., 2003), whereas some other studies reported decreases or no change after generalized seizures (Nitsch et al., 1983; Maciejak et al., 2010; Segovia Porrás et al., 1997). One reason for the inconsistency of

the results could be due to the usage of tissue homogenates (i.e. not microdialysates) which include cytosolic components. Nevertheless, the decrease of the glutamate level in the current study, as assessed with microdialysis, appears to be paradoxical. The different outcome between the current study and previous microdialysis studies could be explained by the method by which transmitter release is induced. Given that cortical and thalamic glutamatergic innervations to MSNs are almost equal in synaptic contacts in mice (Doig et al., 2010), both local neurostimulant infusion and generalized seizures would result in glutamate release from both cortical and thalamic afferents. Of note, c-Fos activity was not elevated by the 4-AP-induced cortical seizures in the parafascicular nucleus, one of the main thalamic nuclei that projects to the striatum (Fig. 5). Therefore, cortical seizures would predominantly trigger glutamate release from cortico-striatal axons, resulting in less glutamate release, which could be handled by an increased capability of glial glutamate uptake, as explained below.

One potential scenario for the concomitant increase of the GABA level and decrease of the glutamate level is an elevation of the surface expression of glutamate transporters that increases the extracellular glutamate uptake capacity. Indeed we have shown that the two major glial high-affinity glutamate transporters GLAST and GLT-1 exhibit such a tendency. As this change takes place in a relatively short time (i.e. approx. 60 min), it is likely that internalized glutamate transporters were recruited to the surface in an activity-dependent manner, rather than *de novo* transcription and translation. For instance, glutamate-induced membrane trafficking of GLAST has been shown in astrocyte primary culture (Duan et al., 1999). Activity-dependent short-term membrane trafficking of GLT-1 is yet to be reported. Interestingly, GLT-1 has been demonstrated to form clusters to enhance the glutamate uptake efficiency. (Zhou and Sutherland, 2004; Nakagawa et al., 2008).

Another possibility is that the astrocytic coverage of glutamatergic synapses increases after elevated cortical activity, restricting extrasynaptic spillover of glutamate. In fact, peri-synaptic astrocytic processes shape the temporal aspects of synaptic transmission (Pannasch et al., 2014) and astrocytes in epileptic patients' brain tend to enlarge their morphology (Oberheim et al., 2008). Moreover, elevated whisker activity for one day has been shown to increase the astrocytic coverage of spine synapses in the mouse barrel cortex, as well as GLT-1 and GLAST protein amounts (Genoud et al., 2006).

Interestingly, the motility of GLT-1 has recently been shown to be regulated by neuronal activity and the extracellular level of glutamate (Murphy-Royal et al., 2015). Together with the surface glutamate transporter increases, these adaptive mechanisms conceivably contribute to protect neurons from excitotoxicity.

Alanine increase after generalized seizures in the homogenates of various parts of the brain including the caudate and putamen has been reported in a previous study (Nitsch et al., 1983). The progressive increase of striatal alanine in the microdialysate is consistent with earlier reports (Morales-Villagrán and Tapia, 1996; Kovács et al., 2003). Moreover, our results demonstrate that alanine is accumulated in the extracellular space. In the muscle, alanine is synthesized from pyruvate by alanine transaminase and released into the circulation to be taken up by the liver, thereby forming the glucose-alanine-cycle. Alanine transaminase is expressed in the brain in mice (Jadhao et al., 2004), rats (Yang et al., 2009), and humans (Yang et al., 2002). *In vivo* utilization of extracellular alanine in the striatum remains to be elucidated. Alanine could be synthesized in neurons and shuttled to astrocytes to carry nitrogen to provide ammonia for glutamine synthesis (Waagepetersen et al., 2000; Zwingmann et al., 2000). On the other hand, neuronal-activity-dependent astrocytic glycolysis produces pyruvate (Pellerin and Magistretti, 1994) and possibly promotes alanine production as the alanine transaminase works on pyruvate (for a possible scheme, Zwingmann et al., 2001). For instance, in honeybee retina, glial alanine has been proposed to be shuttled to neurons to derive pyruvate for the tricarboxylic acid (TCA) cycle (Tsacopoulos et al., 1994). Perhaps the alanine shuttle system has an advantage of preventing acidification of the extracellular medium compared with the lactate shuttle system. Further studies are needed to identify the origin and usage of the extracellular alanine.

References

- Ade KK, Janssen MJ, Ortinski PI, Vicini S (2008) Differential tonic GABA conductances in striatal medium spiny neurons. *J Neurosci* 28:1185–1197.
- Aida T, Yoshida J, Nomura M, Tanimura A, Iino Y, Soma M, Bai N, Ito Y, Cui W, Aizawa H, Yanagisawa M, Nagai T, Takata N, Tanaka KF, Takayanagi R, Kano M, Götz M, Hirase H, Tanaka K (2015) Astroglial Glutamate Transporter Deficiency

Increases Synaptic Excitability and Leads to Pathological Repetitive Behaviors in Mice. *Neuropsychopharmacology*.

- Banerjee PN, Filippi D, Allen Hauser W (2009) The descriptive epidemiology of epilepsy-a review. *Epilepsy Res* 85:31–45.
- Barone P, Morelli M, Cicarelli G, Cozzolino A, DeJoanna G, Campanella G, DiChiara G (1993) Expression of c-fos protein in the experimental epilepsy induced by pilocarpine. *Synapse* 14:1–9.
- Chuhma N, Tanaka KF, Hen R, Rayport S (2011) Functional connectome of the striatal medium spiny neuron. *J Neurosci* 31:1183–1192.
- Doig NM, Moss J, Bolam JP (2010) Cortical and thalamic innervation of direct and indirect pathway medium-sized spiny neurons in mouse striatum. *J Neurosci* 30:14610–14618.
- Duan S, Anderson CM, Stein BA, Swanson RA (1999) Glutamate Induces Rapid Upregulation of Astrocyte Glutamate Transport and Cell-Surface Expression of GLAST. *J Neurosci* 19:10193–10200.
- Genoud C, Quairiaux C, Steiner P, Hirling H, Welker E, Knott GW (2006) Plasticity of astrocytic coverage and glutamate transporter expression in adult mouse cortex. *PLoS Biol* 4:e343.
- Gerfen CR (2004) Basal Ganglia. In: *The Rat Nervous System, Third Edit.* (Paxinos G, ed), pp 455–508. Elsevier Academic Press.
- Grillner S, Hellgren J, Ménard A, Saitoh K, Wikström MA (2005) Mechanisms for selection of basic motor programs--roles for the striatum and pallidum. *Trends Neurosci* 28:364–370.
- Hedreen JC (1977) Corticostriatal cells identified by the peroxidase method. *Neurosci Lett* 4:1–7.
- Hensch TK, Fagiolini M, Mataga N, Stryker MP, Baekkeskov S, Kash SF (1998) Local GABA circuit control of experience-dependent plasticity in developing visual cortex. *Science* 282:1504–1508.
- Hersch S, Ciliax B, Gutekunst C, Rees H, Heilman C, Yung K, Bolam J, Ince E, Yi H, Levey A (1995) Electron microscopic analysis of D1 and D2 dopamine receptor proteins in the dorsal striatum and their synaptic relationships with motor corticostriatal afferents. *J Neurosci* 15:5222–5237.
- Jadhao SB, Yang R-Z, Lin Q, Hu H, Anania FA, Shuldiner AR, Gong D-W, Jadhao SB (2004) Murine alanine aminotransferase: cDNA cloning, functional expression, and differential gene regulation in mouse fatty liver. *Hepatology* 39:1297–1302.

- Jones EG, Coulter JD, Burton H, Porter R (1977) Cells of origin and terminal distribution of corticostriatal fibers arising in the sensory-motor cortex of monkeys. *J Comp Neurol* 173:53–80.
- Kennedy RT, Thompson JE, Vickroy TW (2002) In vivo monitoring of amino acids by direct sampling of brain extracellular fluid at ultralow flow rates and capillary electrophoresis. *J Neurosci Methods* 114:39–49.
- Kovács A, Mihály A, Komáromi Á, Gyengési E, Szenté M, Weiczner R, Krisztin-Péva B, Szabó G, Telegdy G (2003) Seizure, neurotransmitter release, and gene expression are closely related in the striatum of 4-aminopyridine-treated rats. *Epilepsy Res* 55:117–129.
- Lada MW, Vickroy TW, Kennedy RT (1998) Evidence for Neuronal Origin and Metabotropic Receptor-Mediated Regulation of Extracellular Glutamate and Aspartate in Rat Striatum In Vivo Following Electrical Stimulation of the Prefrontal Cortex. *J Neurochem* 70:617–625.
- Luhmann HJ, Dzhala VI, Ben-Ari Y (2000) Generation and propagation of 4-AP-induced epileptiform activity in neonatal intact limbic structures in vitro. *Eur J Neurosci* 12:2757–2768.
- Maciejak P, Szyndler J, Turzyńska D, Sobolewska A, Bidziński A, Kołosowska K, Płaźnik A (2010) Time course of changes in the concentrations of amino acids in the brain structures of pentylenetetrazole-kindled rats. *Brain Res* 1342:150–159.
- Mataga N, Imamura K, Watanabe Y (1991) 6R-tetrahydrobiopterin perfusion enhances dopamine, serotonin, and glutamate outputs in dialysate from rat striatum and frontal cortex. *Brain Res* 551:64–71.
- Morales-Villagrán A, Tapia R (1996) Preferential stimulation of glutamate release by 4-aminopyridine in rat striatum in vivo. *Neurochem Int* 28:35–40.
- Murphy-Royal C, Dupuis JP, Varela JA, Panatier A, Pinson B, Baufreton J, Groc L, Oliet SHR (2015) Surface diffusion of astrocytic glutamate transporters shapes synaptic transmission. *Nat Neurosci* 18:219–226.
- Nakagawa T, Otsubo Y, Yatani Y, Shirakawa H, Kaneko S (2008) Mechanisms of substrate transport-induced clustering of a glial glutamate transporter GLT-1 in astroglial-neuronal cultures. *Eur J Neurosci* 28:1719–1730.
- Nitsch C, Schmude B, Haug P (1983) Alterations in the Content of Amino Acid Neurotransmitters Before the Onset and During the Course of Methoxyypyridoxine-Induced Seizures in Individual Rabbit Brain Regions. *J Neurochem* 40:1571–1580.

- Oberheim NA, Tian GF, Han X, Peng W, Takano T, Ransom B, Nedergaard M (2008) Loss of astrocytic domain organization in the epileptic brain. *J Neurosci* 28:3264–3276.
- Pannasch U, Freche D, Dallérac G, Ghézali G, Escartin C, Ezan P, Cohen-Salmon M, Benchenane K, Abudara V, Dufour A, Lübke JHR, Déglon N, Knott G, Holcman D, Rouach N (2014) Connexin 30 sets synaptic strength by controlling astroglial synapse invasion. *Nat Neurosci* 17:549–558.
- Pellerin L, Magistretti PJ (1994) Glutamate uptake into astrocytes stimulates aerobic glycolysis: a mechanism coupling neuronal activity to glucose utilization. *Proc Natl Acad Sci U S A* 91:10625–10629.
- Peña F, Tapia R (2000) Seizures and neurodegeneration induced by 4-aminopyridine in rat hippocampus in vivo: role of glutamate- and GABA-mediated neurotransmission and of ion channels. *Neuroscience* 101:547–561.
- Rowley HL, Martin KF, Marsden CA (1995) Decreased GABA release following tonic-clonic seizures is associated with an increase in extracellular glutamate in rat hippocampus in vivo. *Neuroscience* 68:415–422.
- Segovia G, Porrás A, Mora F (1997) Effects of 4-Aminopyridine on Extracellular Concentrations of Glutamate in Striatum of the Freely Moving Rat. *Neurochem Res* 22:1491–1497.
- Timmerman W, Westerink BH (1997) Brain microdialysis of GABA and glutamate: what does it signify? *Synapse* 27:242–261.
- Tsacopoulos M, Veuthey AL, Saravelos SG, Perrottet P, Tsoupras G (1994) Glial cells transform glucose to alanine, which fuels the neurons in the honeybee retina. *J Neurosci* 14:1339–1351.
- Waagepetersen HS, Sonnewald U, Larsson OM, Schousboe A (2000) A possible role of alanine for ammonia transfer between astrocytes and glutamatergic neurons. *J Neurochem* 75:471–479.
- Willoughby JO, Mackenzie L, Medvedev A, Hiscock JJ (1995) Distribution of Fos-positive neurons in cortical and subcortical structures after picrotoxin-induced convulsions varies with seizure type. *Brain Res* 683:73–87.
- Wilson CM (2004) Basal Ganglia. In: *The Synaptic Organization of the Brain*, 5th Editio. (Shepherd GM, ed), pp 361–414. Oxford, UK: Oxford University Press.
- Yamaguchi S, Rogawski MA (1992) Effects of anticonvulsant drugs on 4-aminopyridine-induced seizures in mice. *Epilepsy Res* 11:9–16.

Yang R-Z, Blaileanu G, Hansen BC, Shuldiner AR, Gong D-W (2002) cDNA cloning, genomic structure, chromosomal mapping, and functional expression of a novel human alanine aminotransferase. *Genomics* 79:445–450.

Yang R-Z, Park S, Reagan WJ, Goldstein R, Zhong S, Lawton M, Rajamohan F, Qian K, Liu L, Gong D-W (2009) Alanine aminotransferase isoenzymes: molecular cloning and quantitative analysis of tissue expression in rats and serum elevation in liver toxicity. *Hepatology* 49:598–607.

Zhou J, Sutherland ML (2004) Glutamate transporter cluster formation in astrocytic processes regulates glutamate uptake activity. *J Neurosci* 24:6301–6306.

Zwingmann C, Richter-Landsberg C, Brand A, Leibfritz D (2000) NMR spectroscopic study on the metabolic fate of [3-(13)C]alanine in astrocytes, neurons, and cocultures: implications for glia-neuron interactions in neurotransmitter metabolism. *Glia* 32:286–303.

Zwingmann C, Richter-Landsberg C, Leibfritz D (2001) 13C isotopomer analysis of glucose and alanine metabolism reveals cytosolic pyruvate compartmentation as part of energy metabolism in astrocytes. *Glia* 34:200–212.

Figure legends

Figure 1

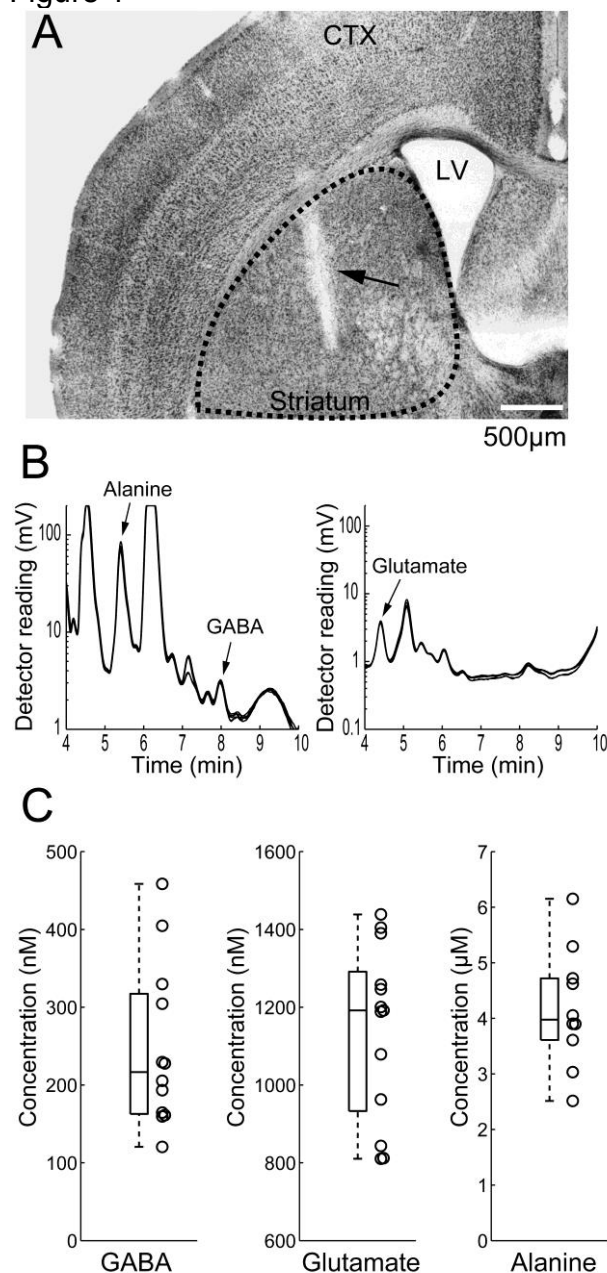


Figure 1. Determination of basal levels of extracellular amino acids in the striatum.

A. Photomicrograph of a Nissl-stained coronal section demonstrating representative microdialysis probe placement (arrow) with a 1-mm active area in the mouse striatum, which is enclosed by a dotted line. CTX, cortex; LV, lateral ventricle.

B. Representative chromatogram of OPA derivatives of free amino acids, GABA and alanine (left panel) or glutamate (right panel), in the extracellular fluid of mouse striatum before 4-AP application. Each line is obtained from an individual animal ($n = 5$) during resting condition. Note that the ordinate axes are shown in logarithmic scale.

C. Distribution of measured basal extracellular levels of GABA, glutamate, and alanine. Rectangles on the left denote the interquartile range (IQR) between the first and third quartiles (25th and 75th percentiles, respectively), and the line inside the boxes denote the median. The dotted whiskers denote the lowest and highest values within 1.5 times the IQR from the first and third quartiles, respectively. Individual data points (per animal) are plotted next to the box plot with circles.

Figure 2

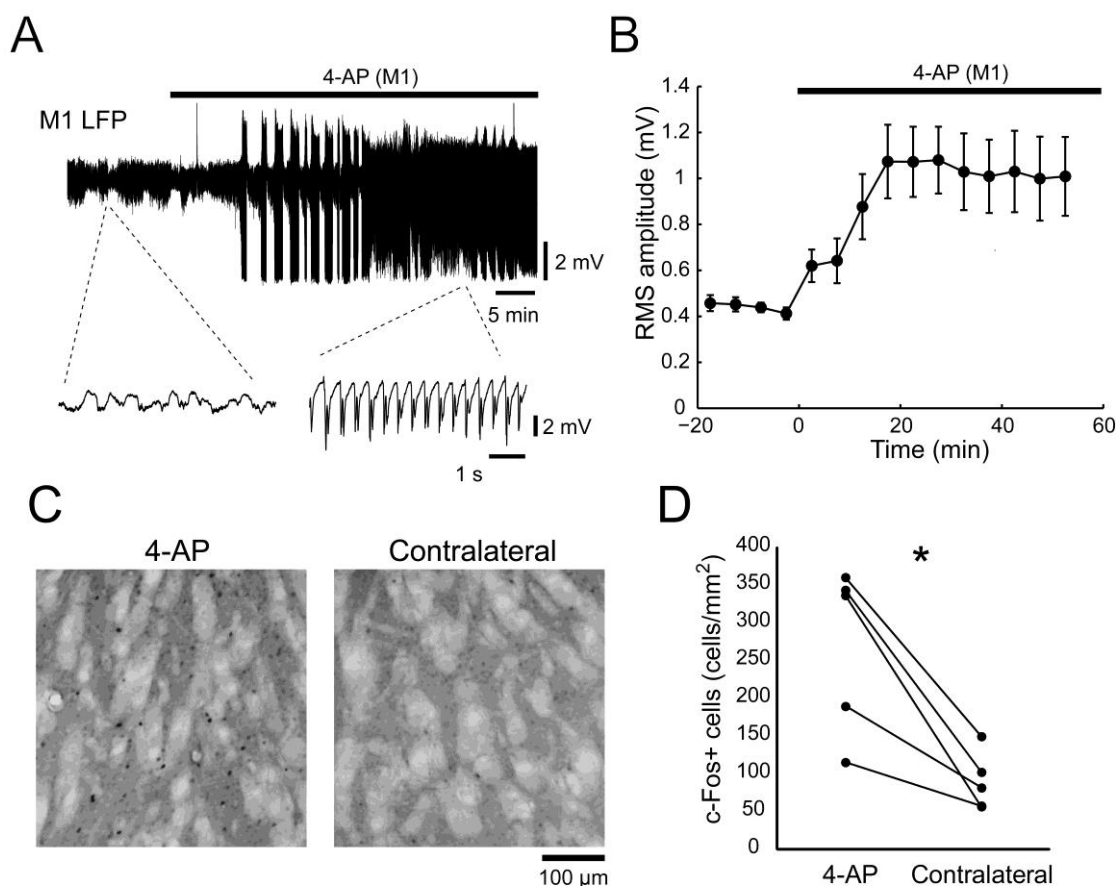


Figure 2. Seizure induction by topical 4-AP application on the motor cortex.

A. Representative LFP responses to topical application of 50 mM 4-AP on the primary motor cortex (M1). Dotted lines indicate the expanded views of LFP before and after 4-AP application.

B. Time-course of the root mean square (RMS) LFP amplitude of the primary motor cortex upon topical 4-AP application. The RMS amplitude doubled and reached at a plateau state 20 min after 4-AP application. Error bars represent \pm S.E.M.

C. Representative photomicrograph of c-Fos immunohistochemistry in the striatum. The striatum of the seizure induction side (4-AP) showed a significantly higher density of c-Fos expression than the contralateral side.

D. c-Fos positive cell density in the striatum was compared for seizure induction side (4-AP) vs. contralateral side to demonstrate that the seizure side has an elevated c-Fos activity. * $p < 0.05$.

Figure 3

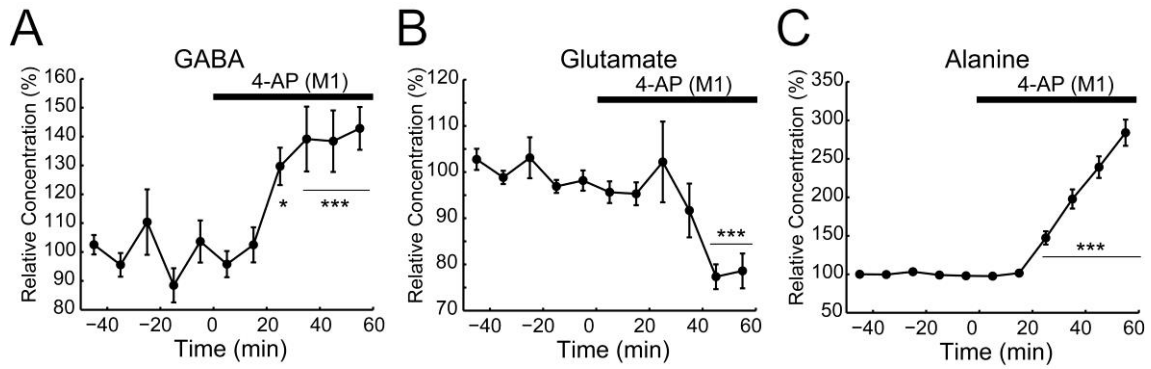


Figure 3. Time course of extracellular amino acid level changes in the striatum after ipsilateral 4-AP-induced motor cortex (M1) seizures.

A. Time course of the GABA level. The GABA level started to increase 20 min after 4-AP application on the motor cortex and reached to a presumable plateau of 143%.

B. Glutamate level decreased to 79% 50 min after motor cortex seizure induction.

C. Alanine concentration increased linearly within 20 min after motor cortex seizure induction.

Statistical significance: * $p < 0.05$, *** $p < 0.001$. Error bars represent \pm S.E.M.

Figure 4

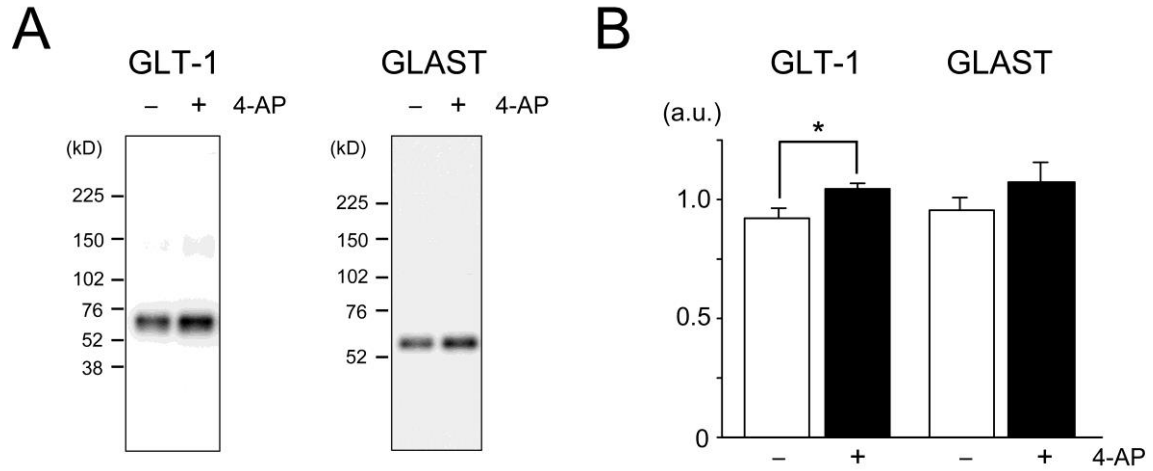
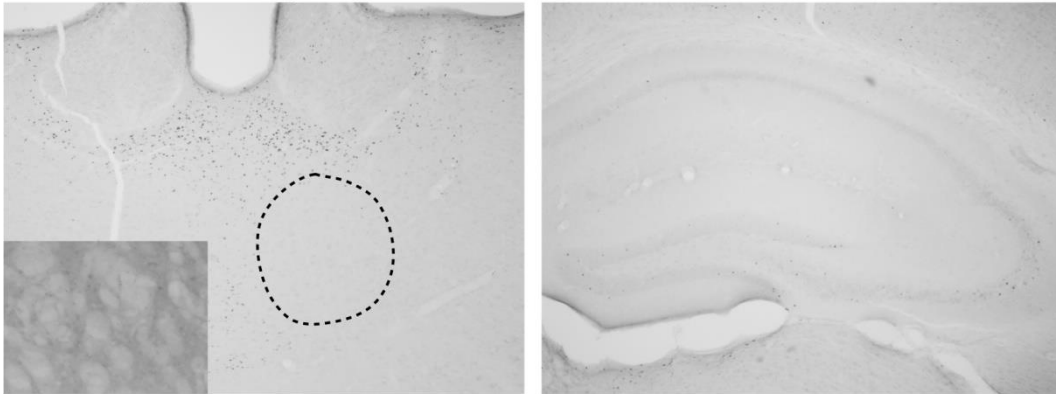


Figure 4. Quantitative immunoblotting of glutamate transporters from mouse striatal membrane fraction with 4-AP treatment

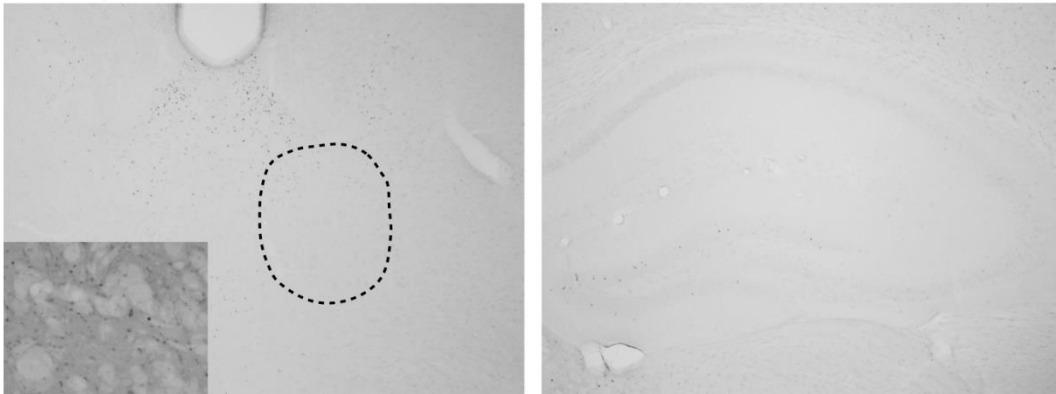
A. Representative GLT-1 and GLAST immunoblots of striatal membrane fraction. The same quantity of membrane fraction protein (220 ng) was prepared and analyzed from control (-) and 4-AP treated (+) mice. The scale for molecular weight (in kD) is indicated on the left side of each blot.

B. Quantification of GLT-1 and GLAST immunoreactive bands measured from six control (-) vs. six 4-AP treated (+) mice. Treatment of 4-AP resulted in a significant elevation of immunoreactivity of GLT-1 ($p = 0.03$). A similar tendency was observed for GLAST, but the difference was not significant ($p = 0.26$). Error bars represent \pm S.E.M.

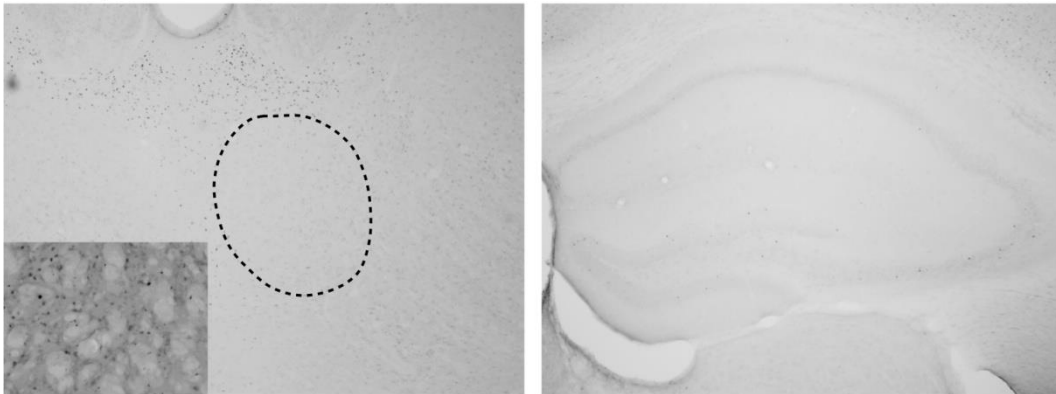
Figure 5
Control (Animal 1)



4-AP (Animal 2)



4-AP (Animal 3)



500 μ m
(250 μ m)

500 μ m

Figure 5. c-Fos expression is not induced in the parafascicular nucleus (PF, left column) or hippocampus (right column) after 4-AP application on the motor cortex. The dotted areas represent approximate locations of the thalamic PF. Inset: c-Fos staining of the striatum of the same animal (magnified). All images are taken from the craniotomy side (i.e. 4-AP side for Animal 2 and 3).